

UL e-ICIC Scheme Using SLP-ABS for Self-Organized Heterogeneous Cellular Networks

Hyung Yeol Lee, *Student Member, IEEE*, Jin Bae Park, *Student Member, IEEE*, and Kwang Soon Kim, *Senior Member, IEEE*

Abstract—In this paper, an uplink (UL) enhanced intercell interference coordination (e-ICIC) scheme using synchronously configured low-power almost blank subframes (SLP-ABSs) is proposed for providing as efficient UL load balancing as in the downlink (DL) of a self-organized heterogeneous cellular network (SO-HCN). An analytical framework is provided as a theoretical background for a successful load balancing, and it is shown that the derived SIR distributions are quite close to the true ones in a wide range of network parameters so that it can be utilized for a successful load balancing. From the simulation results, it is shown that the proposed UL e-ICIC scheme can provide similar load balancing capability as the DL counterpart.

Index Terms—HCN, load balancing, uplink (UL) enhanced ICIC.

I. INTRODUCTION

DEPLOYING of small-cell BSs (tier- s BSs) on existing macro-cell BSs (tier- m BSs), called an HCN, can be an attractive solution for cost-effectively handling the exponentially growing data-traffic demand. In order to provide better quality of service to users, an appropriate load balancing scheme with a cross-tier interference mitigation is required, which brings the cell range expansion combined with the e-ICIC using ABS in the 3GPP long term evolution advanced (LTE-A) [1]. In addition, for utilizing the full potential of an HCN, a low-power transmission during ABSs may be allowed [2]. However, the ABS pattern and allowed power should be tightly controlled, which brings the necessity of a network-wide self organization, i.e., SO-HCN [3]. Among possible candidates, the e-ICIC scheme using SLP-ABS [2], [4], in which the common ABS pattern as well as the amount of power reduction of all tier- m BSs are determined by a central controller, such as the mobility management entity (MME) in the core network, can be considered as a good SO-HCN solution for a network provider. To make the best use of such an SO-HCN for a given load balancing goal, understanding on the link characteristics according to tier, association rule, power control, and resource partitioning is essential. For DL, an analytical framework for a resource partitioning scheme was already given in [5], which

can be easily extended to the case of DL e-ICIC scheme using SLP-ABS. Thus, such an SO-HCN using the DL e-ICIC scheme is ready to be implemented using the current LTE-A standard. However, although UL is as important as DL for user experience, current UL load balancing schemes only adjust the power control target of each tier (e.g., [6]) and an enhanced UL load balancing scheme comparable to the DL counterpart has not been considered yet. So, it would be one of the key technology for a successful user experience in an SO-HCN.

In this paper, a UL e-ICIC scheme using SLP-ABS is proposed for providing as efficient UL load balancing as in DL in an SO-HCN. The proposed UL e-ICIC scheme is different to the DL counterpart due to the different interference characteristics in DL and UL in the sense that i) ABS is applied to tier- s BSs and ii) reducing the power control target during the ABSs, while the network architecture and protocol for the DL e-ICIC scheme can be shared. For a successful UL load balancing, an analytical framework is provided by extending the recent results on UL HCN [7] into the case of using the proposed UL e-ICIC, which can provide not only better understanding but also a theoretical background for an SO-HCN.

II. PROPOSED UL e-ICIC SCHEME USING SLP-ABS

In this paper, we focus on a two-tier heterogeneous cellular networks, such as the 3GPP LTE-A, with macro-cells having transmission power of P_m and receiving antenna gain of A_m whose location set is denoted as \mathbf{Y}_m and small-cells having transmission power of P_s and receiving antenna gain of A_s whose location set is denoted as \mathbf{Y}_s . In addition, \mathbf{X} denotes the location set of users who transmit with variable transmit power up to P_u and receive their signals with receiving antenna gain A_u . It is assumed that SON functions are distributed as in [3], in which each tier- s BS $\mathbf{y} \in \mathbf{Y}_s$ reports its information to the nearby tier- m BS and the network controller (e.g., the MME in LTE-A) determines the DL/UL biases for the cell range expansion, the DL/UL ABS patterns, the DL power reduction levels, and the UL power control targets of each tier during normal subframes and ABSs using the information gathered from all tier- m BSs, including those from tier- s BSs. Note that the SON parameters are determined based on long-term informations only so that the computational complexity is not a burden in the network controller.

From now on, we will focus on UL only. Let $\mathbf{y}(\mathbf{x})$ be the associated BS of user \mathbf{x} in UL determined by adopting the best biased received signal power criterion as $\mathbf{y}(\mathbf{x}) = \arg \max_{\mathbf{y} \in \mathbf{Y}} P_u A_y \kappa_y \|\mathbf{x} - \mathbf{y}\|^{-\alpha}$, where $\mathbf{Y} = \mathbf{Y}_m \cup \mathbf{Y}_s$ and $\kappa_y \geq 1$ and A_y , denoting the biasing factor and the antenna gain of BS \mathbf{y} , are assumed to be given as $\kappa_y = \kappa_k$ and $A_y = A_k$ for $\mathbf{y} \in \mathbf{Y}_k$, $k \in \{m, s\}$, respectively. Also, $\mathbf{X}(\mathbf{y}) = \{\mathbf{x} | \mathbf{y}(\mathbf{x}) = \mathbf{y}, \mathbf{x} \in \mathbf{X}\}$ denotes the set of users associated with BS \mathbf{y} . In order to handle the cross-tier interference, the transmission subframes

Manuscript received July 16, 2014; revised October 22, 2014 and October 29, 2014; accepted October 30, 2014. Date of publication November 7, 2014; date of current version January 7, 2015. This work was supported in part by the Basic Science Research Program through the National Research Foundation of Korea funded by the Ministry of Education, Science and Technology under Grant 2014R1A2A2A01007254 and in part by the ICT R&D program of MSIP/IITP under Grant 2014-044-006-004. The associate editor coordinating the review of this paper and approving it for publication was A. Lioumpas.

The authors are with the Department of Electrical and Electronic Engineering, Yonsei University, Seoul 120-749, Korea (e-mail: ks.kim@yonsei.ac.kr).

Color versions of one or more of the figures in this paper are available online at <http://ieeexplore.ieee.org>.

Digital Object Identifier 10.1109/LCOMM.2014.2368551

are assumed to be partitioned into the tier- s ABSs and the normal subframes, whose portions are given as $0 \leq \zeta_a \leq 1$, and $0 \leq \zeta_n = 1 - \zeta_a \leq 1$, respectively.

In UL, the interference characteristic is very different from that of DL as described in [7] and such a UL interference characteristic becomes more severe in tier- m because tier- m users may suffer from stronger interference caused by tier- s users within its BS coverage. Thus, each tier- s user's transmit power needs to be more strictly controlled and tier- s users may be requested to transmit their signals with a lowered power, similarly as tier- m BSs do in DL, if a nearby tier- m BS wants to schedule tier- m users suffering from high cross-tier interference.

The proposed UL e-ICIC scheme using SLP-ABS can be described as follows. The UL transmit power $P_r(\mathbf{x})$ of user $\mathbf{x} \in \mathbf{X}$ using subframe-type $r \in \{n, a\}$ is assumed to be selected among $\mathbf{P} = \{\mu_j P_u | 0 \leq \mu_1 \leq \dots \leq \mu_J = 1\}$ to maintain the average received power at the associated BS $\mathbf{y} \in \mathbf{Y}_k$ above or equal to $\gamma_{k,r}$ [dB], $k \in \{m, s\}$, i.e., the power control target in each tier can be different to control the cross-tier interference and the target during an ABS may be different to that during a normal subframe. For each tier- m BS $\mathbf{y} \in \mathbf{Y}_m$, the users are divided into the two sets $\mathbf{X}_n(\mathbf{y})$ and $\mathbf{X}_a(\mathbf{y}) = \mathbf{X}(\mathbf{y}) - \mathbf{X}_n(\mathbf{y})$ as

$$\mathbf{X}_n(\mathbf{y}) = \left\{ \mathbf{x} | P_u A_m A_v \|\mathbf{x} - \mathbf{y}(\mathbf{x})\|^{-\alpha} \geq P_u A_m \|\mathbf{x} - \bar{\mathbf{y}}\|^{-\alpha} \text{ for } \forall \bar{\mathbf{y}} \in \mathbf{Y}_m, \mathbf{x} \in \mathbf{X}(\mathbf{y}) \right\}, \quad (1)$$

where $0 < A_v < 1$ denotes the virtual loss in the antenna gain used for discriminating tier- m users whether they are near a cell boundary among tier- m BSs or not. Then, each tier- m BS $\mathbf{y} \in \mathbf{Y}_m$ reports its desired ABS portion to the network SON controller. Similarly as in DL, the network controller determines the common UL ABS pattern with the portion $\{\zeta_a, \zeta_n\}$ and informs it to all BSs. Each tier- s BS $\mathbf{y} \in \mathbf{Y}_s$ schedules its users and the scheduled user $\mathbf{x}(\mathbf{y})$ transmits with $P_n(\mathbf{x}(\mathbf{y}))$ during the normal subframes while does with $P_a(\mathbf{x}(\mathbf{y}))$ during the ABSs,

where $\nu \triangleq \gamma_{s,a}/\gamma_{s,n}$ denotes the power control target ratio for ABS. Each tier- m BS \mathbf{y} schedules its users in $\mathbf{X}_n(\mathbf{y})$ during the normal subframes and does the users in $\mathbf{X}_a(\mathbf{y})$ during the ABSs. In both cases, the scheduled user $\mathbf{x}(\mathbf{y})$, $\mathbf{y} \in \mathbf{Y}_m$, transmit with a normally controlled power $P_n(\mathbf{x}(\mathbf{y}))$, i.e., $\gamma_{m,n} = \gamma_{m,a}$. Note that the targets are also determined by the network SON controller.

III. ANALYTICAL FRAMEWORK FOR UL SO-HCN

Let $\Gamma_{\mathbf{y},r}$ denote the UL SIR between BS \mathbf{y} and its selected user $\mathbf{x}(\mathbf{y}) \in \mathbf{X}_r(\mathbf{y})$, $r \in \{n, a\}$, which is given by

$$\Gamma_{\mathbf{y},r} = \frac{P_r(\mathbf{x}(\mathbf{y})) A_{\mathbf{y}} h_{\mathbf{y}\mathbf{y}} \|\mathbf{x}(\mathbf{y}) - \mathbf{y}\|^{-\alpha}}{\sum_{l \in \{m, s\}} I_{l,r}}, \quad (2)$$

where $I_{l,r} = \sum_{\mathbf{y}' \in \mathbf{Y}_l \setminus \mathbf{y}} P_r(\mathbf{x}(\mathbf{y}')) A_{\mathbf{y}'} h_{\mathbf{y}'\mathbf{y}} \|\mathbf{x}(\mathbf{y}') - \mathbf{y}\|^{-\alpha}$. Here, $h_{\mathbf{y}\mathbf{y}'}$ denotes the instantaneous channel gain between the user $\mathbf{x}(\mathbf{y})$ and BS \mathbf{y}' , which is modeled as an exponential random variable with unit mean, and $\alpha > 2$ denotes the path loss exponent. Then, the UL SIR distribution of tier k using subframe-type r is obtained as $S_{k,r}(T) = \mathbf{E}[\mathbb{P}[\Gamma_{\mathbf{y},r} > T] | \mathbf{y} \in \mathbf{Y}_k]$.

For analytical purposes, \mathbf{Y}_m , \mathbf{Y}_s , \mathbf{X} are assumed to be distributed according to homogeneous Poisson point processes (PPPs) with intensities λ_m , λ_s and λ_u , respectively. Also, $\mathbf{X}_{k,r}$ denotes the set of users in tier- k using subframe-type r , i.e., $\mathbf{X}_{k,r} = \bigcup_{\mathbf{y} \in \mathbf{Y}_k} \mathbf{X}_r(\mathbf{y})$. Let ψ_k denote the association probability of a randomly selected user $\mathbf{x} \in \mathbf{X}$ to a tier- k BS and $\psi_{k,r}$ denote

TABLE I
SUMMARY ON THE NOTATIONS

Symbol	Description
k, r	Tier- $k \in \{m, s\}$, subframe-type $r \in \{n, a\}$
$\mathbf{Y}, \mathbf{Y}_k, \mathbf{y}(\mathbf{x})$	Set of BSs, set of BSs in tier- k , associated BS of user \mathbf{x}
$\mathbf{X}, \mathbf{X}_{k,r}$	Set of users, set of users in tier- k using subframe-type r
$\mathbf{X}(\mathbf{y}) (\mathbf{X}_r(\mathbf{y})), \mathbf{x}(\mathbf{y})$	Set of users associated to BS \mathbf{y} (using subframe-type r), the randomly selected user by \mathbf{y}
λ_k, λ_u	Tier- k BS density and user density
A_k, κ_k, A_v	Tier- k antenna gain and biasing factor, the virtual loss
$P_r(\mathbf{x})$	Transmit power of user \mathbf{x} using subframe-type r
$\gamma_{k,r} (\eta_{k,r}), \nu$	Tier- k UL target SNR (power) at subframe-type r , the power control target ratio for ABS
$\zeta_a (\zeta_n)$	Tier- s ABS (normal subframe) portion
$\Gamma_{\mathbf{y},r}$	SIR of the selected user in BS \mathbf{y} using resource r
$S_{k,r}(T)$	Tier- k SIR distribution using subframe-type r
$\psi_k (\psi_{k,r})$	Tier- k association probability (using subframe-type r)
$R_k, f_{R_k}(y \mathbf{x} \in \mathbf{X}_{k,r})$	Distance between a selected user in tier- k and its associated BS, PDF of R_k using subframe-type r

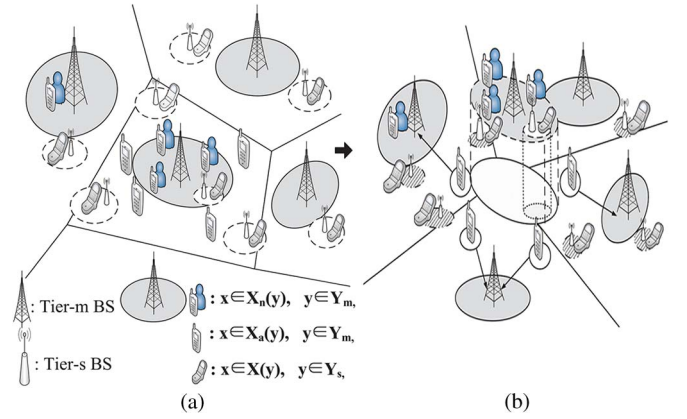


Fig. 1. The association regions for the proposed UL e-ICIC scheme. (a) True HCNs. (b) Virtually divided HCNs.

the association probability of a randomly selected user $\mathbf{x} \in \mathbf{X}$ using subframe-type r of a tier- k BS, i.e., $\psi_{k,r} = \Pr\{\mathbf{x} \in \mathbf{X}_{k,r}\}$. Then, $\psi_k = \sum_{r \in \{n, a\}} \psi_{k,r}$. Also, let R_k denote the distance between a randomly selected user $\mathbf{x} \in \mathbf{X}$ and its associated BS and $f_{R_k}(y | \mathbf{x} \in \mathbf{X}_{k,r})$ denote the distribution of R_k conditioned on $\mathbf{x} \in \mathbf{X}_{k,r}$. The notations used in this paper are summarized in Table I.

The association probabilities $\psi_m = \psi_{m,n} + \psi_{m,a}$ and ψ_s can be obtained as in the DL case [8] with the transmit powers of $P_u A_m / A_u$ and $P_u A_s / A_u$ and the biasing factors of κ_m and κ_s , respectively for tier- m and tier- s . For obtaining the association probability $\psi_{m,n}$, two HCNs are considered as depicted in Fig. 1. The left one denotes the point processes and the corresponding association areas according to the true UL e-ICIC scheme and the right one in Fig. 1(b) is the derived point processes from Fig. 1(a) by i) selecting β portions of BSs in tier- m , ii) re-allocating the outer (non-shaded) area of the selected BSs to other tier- m or tier- s BSs as if the selected BSs do not exist, and iii) shrinking the regions of tier- s BSs in the outside of the selected tier- m BS region (in non-shaded areas) as if the antenna gain is reduced to $A_s A_v$. Then, it becomes a realization of a 3-tier HCN in which tier- m_1 BSs with the density of $(1 - \beta)\lambda_m$ and the antenna gain of A_m , tier- m_2 BSs with the density of $\beta\lambda_m$ and the antenna gain of $A_m A_v$, and tier- s BSs with density of λ_s and the antenna gain of $A_s A_v$. Then, it is apparent that $f_{R_k}(y | \mathbf{x} \in \mathbf{X}_{k,r})$ in Fig. 1(a) is equal to the distribution of R_{m_2} in Fig. 1(b) as $\beta \rightarrow 0$. Also, $\psi_{s,n}$ in Fig. 1(a) is equal to $\psi_{m_2} \beta^{-1}$ as $\beta \rightarrow 0$. Note that $\beta \rightarrow 0$ is required to rule out the interaction

among multiple tier- m_2 BSs in Fig. 1(b), which does not happen in Fig. 1(a).

Lemma 1: The association probabilities $\psi_{k,r}$ and the distributions of $f_{R_k}(y|\mathbf{x} \in \mathbf{X}_{k,r})$ are obtained as

$$\Psi_{m,n} = \frac{1}{\mathcal{M}_{m,n}}, \Psi_{m,a} = \frac{1}{\mathcal{M}_m} - \Psi_{m,n}, \Psi_{s,n} = \frac{1}{\mathcal{M}_s}, \Psi_{s,a} = 0, \quad (3)$$

$$f_{R_m}(y|\mathbf{x} \in \mathbf{X}_{m,n}) = 2\pi\lambda_m \mathcal{M}_{m,n} y e^{-\pi\lambda_m \mathcal{M}_{m,n} y^2}, \quad (4)$$

$$f_{R_s}(y|\mathbf{x} \in \mathbf{X}_{s,n}) = 2\pi\lambda_s \mathcal{M}_s y e^{-\pi\lambda_s \mathcal{M}_s y^2}, \quad (5)$$

$$f_{R_m}(y|\mathbf{x} \in \mathbf{X}_{m,a}) = \frac{\Psi_m}{\Psi_{m,a}} 2\pi\lambda_m y \mathcal{M}_m e^{-\pi\lambda_m \mathcal{M}_m y^2} - \frac{\Psi_{m,n}}{\Psi_{m,a}} 2\pi\lambda_m y \mathcal{M}_{m,n} e^{-\pi\lambda_m \mathcal{M}_{m,n} y^2}, \quad (6)$$

where $\mathcal{M}_k = \hat{\lambda}_{\bar{k},k} \hat{A}_{\bar{k},k}^{2/\alpha} + 1$, $\bar{k} \in \{m, s\} \setminus \{k\}$, $\mathcal{M}_{m,n} = \hat{\lambda}_{s,m} \hat{A}_{s,m}^{2/\alpha} + A_v^{-2/\alpha}$, $\hat{A}_{k,l} = A_k \kappa_k / (A_l \kappa_l)$, and $\hat{\lambda}_{k,l} = \lambda_k / \lambda_l$.

Proof: In Fig. 1(b), $\Psi_{m_2} = 1/\mathcal{M}'(\beta)$ and $f_{m_2}(y) = 2\pi\beta\lambda_m \mathcal{M}'(\beta) x \exp(-\pi\beta\lambda_m \mathcal{M}'(\beta) x^2)$, where $\mathcal{M}'(\beta) = 1 + (1-\beta)\beta^{-1} A_v^{-2/\alpha} + \beta^{-1} \hat{\lambda}_{s,m} \hat{A}_{s,m}^{2/\alpha}$. Thus, $\Psi_{m,n} = \lim_{\beta \rightarrow 0} \Psi_{m_2} \beta^{-1} = 1/\mathcal{M}_{m,n}$ and $f_{R_m}(y|\mathbf{x} \in \mathbf{X}_{m,n}) = \lim_{\beta \rightarrow 0} f_{m_2}(y) = 2\pi\lambda_m \mathcal{M}_{m,n} y \exp(-\pi\lambda_m \mathcal{M}_{m,n} y^2)$. ■

As shown in [7], the UL interferer location distribution and the UL interferer power distribution can be successfully approximated as an independent non-homogeneous PPP for the interferer location distribution and an independent and identically distributed power distribution for each interferer in a tier using the same subframe type regardless of its location. In [7], the tier- l interferer intensity function at (v, θ) to the tier- k BS at the origin is obtained as the probability that an active interferer exists at the point, which is at least one tier- l BS should be located within the circle centered at (v, θ) with radius of $\hat{A}_{k,l}^{-1/\alpha} v$, times the tier- l BS density λ_l . For the UL e-ICIC scheme, the tier- m interference to a tier- k BS changes according to the subframe-type r and the corresponding area for $l = m$ (the circle with radius $\hat{A}_{k,l}^{-1/\alpha} v$) is divided into a smaller concentric circle with radius $(\Psi_{m,a}/\Psi_m)^{1/2} \hat{A}_{k,l}^{-1/\alpha} v$ for $r = n$ and the remaining donut shape for $r = a$ whose area is $\Psi_{m,n}/\Psi_m$ times of the original circle area. Then, similarly as in [7], the interferer location distribution from tier- l to tier- k BS at subframe-type r can be approximated as an independent non-homogeneous PPP with density of $\lambda_{k,l,r}(v) = \lambda_l \min(\delta_{k,l,r} v, 1)$, where $\delta_{k,l,r} = (\pi\lambda_l \Psi_{l,r} / (4\Psi_l))^{1/2} (1 + \hat{A}_{k,l}^{-1/\alpha})^{-0.1} \hat{A}_{k,l}^{1/\alpha}$ if $l = m$, and $\delta_{k,l,r} = (\pi\lambda_l / 4)^{1/2} (1 + \hat{A}_{k,l}^{-1/\alpha})^{-0.1} \hat{A}_{k,l}^{1/\alpha}$, otherwise.

Also, the i.i.d. power distribution for UL interferers in tier- k , $p_{k,r}(j) \triangleq \mathbb{P}[P_r(\mathbf{x}(y)) = \mu_j P_u]$, $j = 1, \dots, J$, can be easily obtained similarly as in [7] by using Lemma 1 as

$$p_{k,r}(j) \simeq \begin{cases} \mathcal{P}(j; \lambda_s \mathcal{M}_s, \eta_{s,r}), & k = s, \\ \mathcal{P}(j; \lambda_m \mathcal{M}_{m,n}, \eta_{m,n}), & (k,r) = (m,n), \\ \frac{\Psi_{m,a}}{\Psi_m} \mathcal{P}(j; \lambda_m \mathcal{M}_m, \eta_{m,a}) & \\ \frac{\Psi_{m,n}}{\Psi_{m,a}} \mathcal{P}(j; \lambda_m \mathcal{M}_{m,n}, \eta_{m,a}), & (k,r) = (m,a), \end{cases} \quad (7)$$

where

$$\mathcal{P}(j; u, x) = \begin{cases} e^{-u \left(\frac{\mu_{j-1} P_u}{x}\right)^{2/\alpha}} - e^{-u \left(\frac{\mu_j P_u}{x}\right)^{2/\alpha}}, & j = 1, \dots, J-1, \\ e^{-u \left(\frac{\mu_{j-1} P_u}{x}\right)^{2/\alpha}}, & j = J, \end{cases}$$

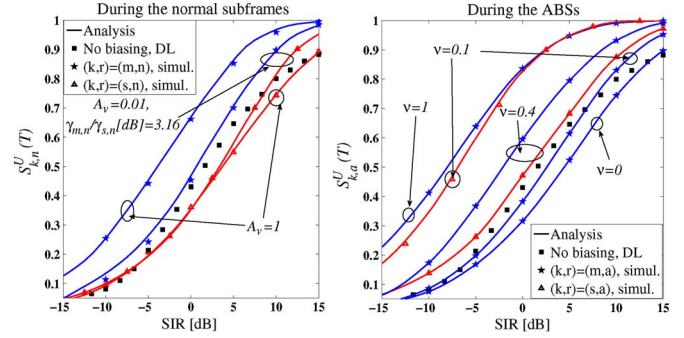


Fig. 2. The UL SIR distributions.

$\mu_0 = 0$, and $\eta_{k,r} = 10^{0.1\gamma_{k,r}} N_0 / A_k$, where N_0 denotes the one-sided noise spectral density.

Theorem 1: The SIR distribution $\mathcal{S}_{k,r}(T)$, for $k \in \{m, s\}$ and $r \in \{n, a\}$, between a randomly selected user $\mathbf{x} \in \mathbf{X}_{k,r}$ and its associated BS is well approximated as

$$\mathcal{S}_{k,r}(T) \simeq \begin{cases} 1 - \mathcal{J}(T; \lambda_s \mathcal{M}_s, \bar{x}_{s,r}, \Delta_{s,r}, \mathbf{P}_r, \Lambda), & k = s, \\ 1 - \mathcal{J}(T; \lambda_m \mathcal{M}_{m,n}, \bar{x}_{m,n}, \Delta_{m,n}, \mathbf{P}_n, \Lambda), & (k,r) = (m,n), \\ 1 - \frac{\Psi_{m,a}}{\Psi_m} \mathcal{J}(T; \lambda_m \mathcal{M}_m, \bar{x}_{m,a}, \Delta_{m,a}, \mathbf{P}_a, \Lambda) \\ + \frac{\Psi_{m,n}}{\Psi_{m,a}} \mathcal{J}(T; \lambda_m \mathcal{M}_{m,n}, \bar{x}_{m,n}, \Delta_{m,a}, \mathbf{P}_a, \Lambda), & (k,r) = (m,a), \end{cases} \quad (8)$$

where $\bar{x}_{k,r} = (P_u / \eta_{k,r})^{1/\alpha}$, $\Delta_{k,r} = [\delta_{k,m,r} \delta_{k,s,r}]$, $\mathbf{P}_r = [p_{m,r} p_{s,r}]$, $\Lambda = [\lambda_m \lambda_s]$ and $\mathcal{J}(T; s, x, \Delta, \mathbf{P}, \Lambda)$ is as defined in [7].

Proof: Note that $1 - \mathcal{J}(T; \lambda_k \mathcal{M}_k, \bar{x}_k, \Delta_k, \mathbf{P}, \Lambda_{k,r})$ denotes the tier- k UL SIR distribution in an HCN ((6) of [7]), where $\lambda_k \mathcal{M}_k = \bar{\lambda}_k \hat{A}_{\bar{k},k}^{2/\alpha} + \lambda_k$ denotes the tier- k heterogeneity parameter for tier- k as can be seen in Lemma 1 and $\bar{x}_k, \mathbf{P}, \Delta_k$, and $\Lambda_{k,r}$ are as defined in [7]. Then, the UL SIR distributions are obtained in the same way as in a plain HCN by applying the following changes. For the interference part, the non-uniform density vector Δ_k is changed to $\Delta_{k,r}$ to reflect the interferer intensity function at subframe-type r . At the same time, \mathbf{P} and \bar{x}_k are changed to \mathbf{P}_r and $\bar{x}_{k,r}$, respectively, in order to reflect the interferer power distribution at subframe-type r . For the desired signal part, $\lambda_s \mathcal{M}_s$ and $\lambda_m \mathcal{M}_{m,n}$ denote the heterogeneity parameters for the cases of $k = s$ and $(k,r) = (m,n)$, respectively, as can be seen in Lemma 1, which concludes the proof for the case of $k = s$ and $(k,r) = (m,n)$. Similarly as in the proof for Theorem 1, $(k,r) = (m,a)$ case is obtained by using (3) and (6). ■

IV. SIMULATION RESULT

For the simulation, macro-cell BSs and users are generated according to PPPs with densities $\lambda_m = 1\text{BS}/(\pi(1.5\text{ km})^2)$ and $\lambda_u = 300\tilde{\lambda}_m$, respectively, over a circle with radius 50 km for each iteration and the SIR values computed using (2) are collected over a circle with radius 10 km.

In Fig. 2, the UL SIR distributions $\mathcal{S}_{k,r}(T)$ obtained from Theorem 1 are compared to those obtained from the simulations for various values of v and A_v when $\hat{\lambda}_{s,m} = 5$ and $\hat{A}_{s,m} = 0.2$. From the results, it is confirmed that the derived UL SIR distributions for the proposed UL e-ICIC scheme using SLP-ABS are well matched to the true SIR distributions. During the normal subframes, the tier- m SIR distribution becomes much

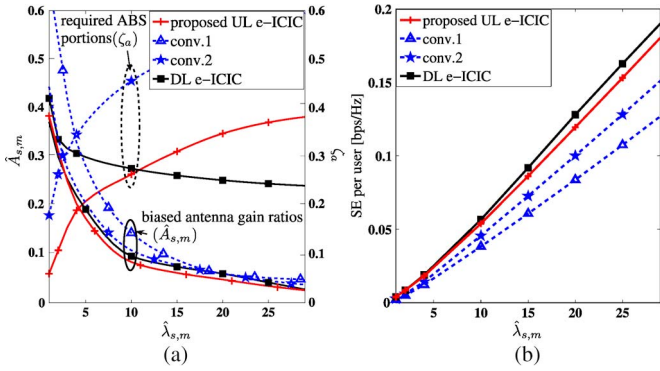


Fig. 3. The load balancing performance comparison in an SO-HCN. (a) The optimal SON parameters. (b) The spectral efficiency per user.

deteriorated in a plain HCN ($A_v = 1$) with the same power control target for both tiers due to the cross-tier interference from tier- s but it can be alleviated by scheduling users in the inner region of tier- m at little cost in tier- s by appropriately adjusting A_v and the power control target ratio between tiers ($\gamma_{m,n}/\gamma_{s,n}$ [dB]). Also, it is shown that the proposed UL e-ICIC scheme can provide good link quality in both tiers comparable to DL during the normal subframes. During the ABSs, the tier- m SIR distribution becomes quite deteriorated if the power control target of tier- s is not reduced ($v = 1$) because users in the outer region of tier- m are scheduled, and it can be handled by using the resource partitioning ($v = 0$) [4]. When the SLP-ABS is applied, tier- s can secure some additional resource with slightly lower quality (compared to DL) at little cost for tier- m ($v = 0.1$) or with enough quality at some cost for tier- m ($v = 0.4$). Note that such a trade-off can be beneficial for satisfying various load balancing criteria.

To evaluate the gain of the proposed UL e-ICIC scheme in a practical system, an LTE-A SO-HCN is considered, in which DL/UL e-ICIC scheme using SLP-ABS is employed and the network SON controller determines the load balancing parameters obtained by utilizing the proposed framework. Here, single-antenna BSs with 10 MHz system bandwidth, the outdoor pico model 1 for tier- s BSs [9], and an independent round-robin scheduling for each resource block (RB) of each subframe using the 5-bit MCS table [10] are assumed. Also, the load balancing target for the SON is set to maximize the average spectral efficiency (SE) per user while satisfying i) similar outage probabilities for both tiers at target SIR T_0 and ii) the average spectral efficiency ratio within L between the two tiers. For the simulation, the channel model is assumed as defined in [9], where the tier- m (tier- s) path-loss exponent is set to $\alpha_m = 3.76$ ($\alpha_s = 3.67$) and the shadowing gain of tier- m (tier- s) is a lognormal distribution with standard deviation of 10 [dB] (8 [dB]). In order to utilize the proposed work, the effective BS density is used for obtaining (8) to include the shadowing effect with a modified approach for the case of different pathloss exponents as described in [7]. After applying the load balancing parameters on the LTE-A SO-HCN, the performance evaluation is done by using the PHY abstraction methodology using the MCS/TBS table [10] on the 100 RBs of each subframe over 10^5 iterations.

In Fig. 3, the optimal SON parameters obtained from the proposed framework as well as the resulting average spectral efficiency per user obtained from the system-level simulation on the LTE-A SO-HCN are plotted according to BS

density ratio $\hat{\lambda}_{s,m}$ when the DL outage probability of 0.2 at $T_0 = -5$ [dB] is used as the reference and $L = 2$. Here, conv.1 and conv.2 denote the case using the DL based association with UL power control only [6], in which only power control is considered without using e-ICIC, and the case using UL-based association with joint UL power control and resource partitioning [7], in which low-power transmission is not allowed during ABSs, respectively. Note that the proposed scheme requires less expansion ($\hat{A}_{s,m}$) than the conventional schemes at the same load balancing target as shown in Fig. 3(a). Also, the required ABS portion (ζ_a) of the proposed scheme is comparable to that in DL while the conventional schemes require much larger ABS portion (conv.2) or much strict power control in tier- s (conv.1). Although not shown explicitly, $\gamma_{m,n}/\gamma_{s,n} = 3.3 \sim 5.3$ [dB] while it is 4.1 \sim 10.8 [dB] (4.3 \sim 6.9 [dB]) in conv.1 (conv.2). Also, not shown explicitly, $v = 0.10 \sim 0.01$ for $\hat{\lambda}_{s,m} = 1 \sim 30$, which implies that less power is allowed during ABSs as the number of tier- s BSs per tier- m BS increases. As can be seen in Fig. 3(b), it is confirmed that the proposed UL e-ICIC scheme using SLP-ABS scheme can provide comparable load balancing capability to the DL e-ICIC scheme in the LTE-A SO-HCN, which cannot be obtained from conventional schemes.

V. CONCLUSION

In this paper, a UL e-ICIC scheme using SLP-ABS is proposed for an SO-HCN by i) applying ABSs to tier- s BSs and ii) reducing the power control target during the ABSs. An analytical framework is proposed and shown to be quite close to the true SIR distributions in a wide range of network parameters. Simulation results show that the proposed UL e-ICIC scheme using SLP-ABS can be successfully utilized to provide good UL load balancing capability comparable to DL in a practical SO-HCN for better user experience.

REFERENCES

- [1] S. Ahmadi, *LTE-Advanced*, 1st ed. New York, NY, USA: Academic, 2013.
- [2] "Considerations on reduced transmission power ABS concept," Zoetermeer, The Netherlands, 3GPP R4-120402, Feb. 2012.
- [3] Small Cell Forum. Urban SON use cases document, Gloucestershire, U.K., SFC077.04.01. [Online]. Available: http://www.scf.io/en/documents/077_-_Urban_SON_use_cases.php
- [4] J. Pang *et al.*, "Optimized time-domain resource partitioning for enhanced inter-cell interference coordination in heterogeneous networks," in *Proc. IEEE Wireless Commun. Netw. Conf.*, Shanghai, China, Apr. 2012, pp. 1613–1617.
- [5] S. Singh and J. G. Andrews, "Joint resource partitioning and offloading in heterogeneous networks," *IEEE Trans. Wireless Commun.*, vol. 13, no. 2, pp. 888–901, Feb. 2014.
- [6] J. Liu *et al.*, "Uplink power control and interference coordination for heterogeneous networks," in *Proc. IEEE 23rd Int. Symp. Pers. Indoor Mobile Radio Commun.*, Sydney, Australia, Sep. 2012, pp. 519–523.
- [7] H. Y. Lee, Y. J. Sang, and K. S. Kim, "On the uplink SIR distributions in heterogeneous cellular networks," *IEEE Commun. Lett.*, vol. 18, no. 12, pp. 2145–2148, Dec. 2014.
- [8] H. Jo, Y. J. Sang, P. Xia, and J. G. Andrews, "Heterogeneous cellular networks with flexible cell association: A comprehensive downlink SINR analysis," *IEEE Trans. Wireless Commun.*, vol. 11, no. 10, pp. 3484–3495, Oct. 2012.
- [9] "Evolved universal terrestrial radio access: Further advancements for E-UTRA physical layer aspects (at Annex A)," Sophia-Antipolis Cedex, France, 3GPP TR 36.814, Mar. 2010.
- [10] "TBS and MCS signaling and tables," Schaumburg, IL, USA, 3GPP R1-0881638, Apr. 2008.